

Analysis of Steel Refining in Pony Ladle

V. G. Efimova*

National Technical University of Ukraine @Igor Sikorsky Kyiv Polytechnic Institute, Kyiv, 03056 Ukraine

*e-mail: chief@nomit.ru

Received April 14, 2020

Abstract—The basic laws of ballistic motion are used to calculate the following in coordinate form: the residence time of a metal droplet in slag with adsorbed nonmetal impurities (NMIs) with the inert gas blowing of liquid steel in a CC machine's pony ladle. These data can be used to set the optimal speed of eliminating NMIs from the metal in the pony ladle at different gas consumption rates, as well as the plausible diameter of gas bubbles. The eliminations of the NMIs in the pony ladle using extended blowoff tuyeres were compared for efficiency during industrial tests. The NMI content was estimated by technique K4 under DIN 50602-1985. The theoretical calculation of the optimal inert gas consumption for the metal blowoff through an extended multichannel tuyere was made, the surpassing of which weakens the refining effect due to the slag capture in liquid melt.

Keywords: pony ladle, CC machine, nonmetal impurities, residence time, extended blowoff tuyere, slag phase, refining

DOI: 10.3103/S0967091220060029

The steel contamination with nonmetal impurities is an important indicator of its quality [1–5]. NMIs are efficiently eliminated by blowing off liquid steel melt with inert gas in the industrial ladle of a CC machine [6–9].

The design features of modern pony ladles allow coagulating NMIs thanks to a pattern of metal stream propagation at blowoff. The optimal pony ladle design, as well as the efficiency of blowoff parameters, depends on the process specs of a particular CC machine.

FORMULATION OF THE PROBLEM

The NMI content is the main indicator of the cast product quality. It is important to note that the direct sampling for analyzing specimens of the liquid melt–slag–NMI system does not seem possible. During the inert gas blowoff of steel, the argon bubbles catch the metal drops with NMIs and are then carried away into the slag phase, where the NMI are adsorbed by the slag [10–12]. Thus, the pattern and number of eliminated impurities remain understudied and several researchers [13, 14] assume that the driving force behind this process is the metal film rupture of the argon bubble.

This paper is aimed at studying the behavior of metal drops in slag, defining their residence time of existence and the dispersed metal weight.

RESEARCH METHOD

The motion path of a single droplet of iron in the slag phase was defined using the ballistic motion law in coordinate form [15]. For the motion pattern of a metal droplet with NMIs in the slag phase, see Fig. 1.

Assuming that the slag phase is stationary, the balance of vertical (coordinate z) and horizontal (coordinate r) forces can be recorded as in [15]:

$$\rho_{\text{dr}} V_{\text{dr}} \frac{du_z}{d\tau} = F_{\text{lf}} - F_{\text{gr}} - F_{\text{res}} - F_{\text{A}}, \quad (1)$$

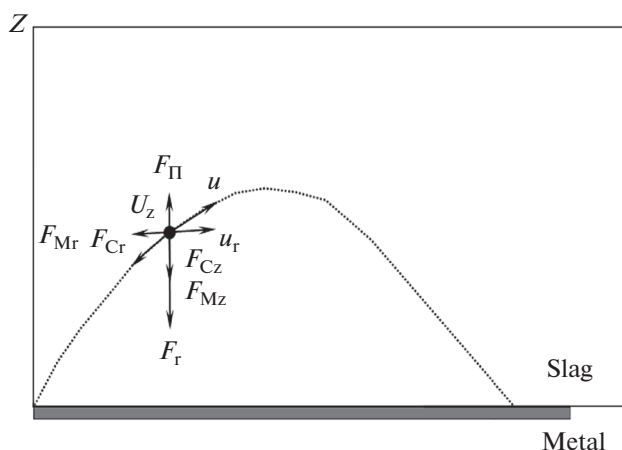


Fig. 1. Motion pattern of a metal droplet with attached impurities in slag phase

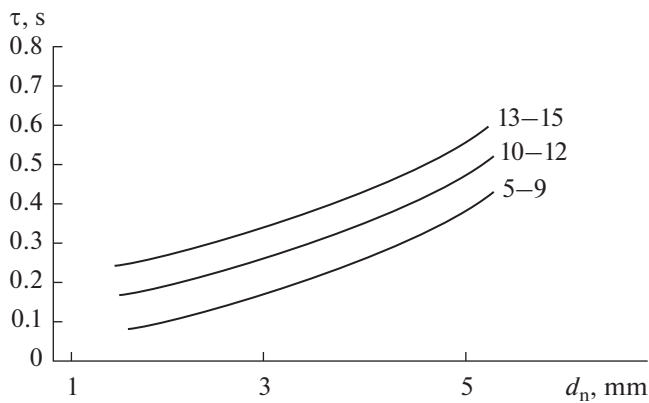


Fig. 2. Influence of bubble diameter d_n and the gas consumption on the residence time of a metal droplet in the slag phase; the numbers near the curves are for the gas consumption in L/min

for direction z
and

$$\rho_{\text{dr}} V_{\text{dr}} \frac{du_r}{d\tau} = -F_{\text{res}} - F_A, \quad (2)$$

for direction r , where F_{lf} , F_{gr} , F_{res} , F_A are the lifting force, gravitation, resistance, and attached weight, respectively; V_{dr} is the droplet volume in m^3 ; ρ is the droplet density in kg/m^3 ; u_z and u_r are the metal droplet motion speeds in directions z and r , respectively, m/s ; τ is the time in s .

The respective forces can be expressed as

$$\begin{aligned} F_{\text{lf}} &= V_{\text{dr}} \rho_{\text{sl}} g, & F_{\text{gr}} &= V_{\text{dr}} \rho_{\text{dr}} g, \\ F_{\text{res},z} &= \frac{1}{2} A_{\text{dr}} C_{kz} \rho_{\text{sl}} u_z^2, & F_{\text{res},r} &= \frac{1}{2} A_{\text{dr}} C_{kr} \rho_{\text{sl}} u_r^2, \\ F_{A,z} &= \frac{1}{2} A_k V_k \rho_{\text{sl}} \frac{du_z}{d\tau}, & F_{A,r} &= \frac{1}{2} A_k V_k \rho_{\text{sl}} \frac{du_r}{d\tau}, \end{aligned}$$

where ρ_{sl} is the slag density in kg/m^3 ; g is the gravitational constant in m/s^2 ; A_{dr} is the droplet area in m^2 ; u_z and u_r are the metal droplet motion speeds in directions z and r , respectively, m/s ; C_k is the head drag coefficient defined as $C_k = 24 N_{\text{Re}}^{-1}$ ($N_{\text{Re}} \leq 1$), where Reynold's numbers N_{Re} in directions z and r are defined as

$$N_{\text{Re},z} = \frac{\rho_{\text{sl}} u_z D_{\text{dr}}}{\mu_{\text{sl}}}, \quad (3)$$

$$N_{\text{Re},r} = \frac{\rho_{\text{sl}} u_r D_{\text{dr}}}{\mu_{\text{sl}}}, \quad (4)$$

where D_{dr} is the droplet diameter in m ; μ_{sl} is slag viscosity, Pa/s .

The droplet motion path in directions z and r can be calculated as

$$L_z(i) = \sum_i \frac{1}{2} [u_z(i) + u_z(i-1)] \Delta\tau, \quad (5)$$

$$L_r(i) = \sum_i \frac{1}{2} [u_r(i) + u_r(i-1)] \Delta\tau. \quad (6)$$

The refining process starts when the drops with NMIs fall into the slag. They leave the slag after the process. The residence time is a timespan in which the metal droplet remains in the slag phase.

Considering the foregoing, the residence time of the droplet in the slag can be recorded as

$$\tau = \sum_i \Delta\tau. \quad (7)$$

The impurity content in the droplet is defined as the amount of impurities assimilated by the slag in time:

$$[\% \text{ wt NMI}] = a(1 + e^{-k\tau}), \quad (8)$$

where $[\% \text{ wt. NMI}]$ is the NMI content per droplet; a and k are the constants of 1.47 and 0.313, respectively, borrowed from work [5]. In this case, the refining rate can be recorded as

$$V_{\text{ref}} = -\frac{d[\% \text{ wt NMI}]}{d\tau} = ake^{-k\tau}. \quad (9)$$

Considering that the heterogeneous reactions observed at the phase boundary are of the first order, the NMI assimilation rate using the residence time data can be recorded as

$$\begin{aligned} V_{\text{ref}} &= -\frac{[\% \text{ wt NMI}]}{d\tau} \\ &= k_{\text{eff}} \frac{A_{\text{dr}}}{V_{\text{dr}}} ([\% \text{ wt NMI}] - [\% \text{ wt. NMI}]_{\text{eq}}), \end{aligned} \quad (10)$$

where $[\text{wt } \% \text{ NMI}]_{\text{eq}}$ is the equilibrium content of NMIs; k_{eff} is the effective chemical reaction speed constant in s^{-1} , defined as

$$k_{\text{eff}} = 2 \sqrt{\frac{D_{\text{NMI}} u_{\text{dr}}}{\pi D_{\text{dr}}}}, \quad (11)$$

where D_{NMI} is the coefficient of NMI in liquid Fe, m^2/s ; u_{dr} is the droplet motion speed in m/s .

RESULTS AND DISCUSSION

The exposed approach was used for defining the residence time of metal droplets in the slag phase at different inert gas consumption rates and bubble diameters (Fig. 2). According to Fig. 2, the bigger is the bubble diameter and the higher is the gas consumption, the longer is the residence time of the metal droplet in the slag phase, which favorably affects the metal refining process.

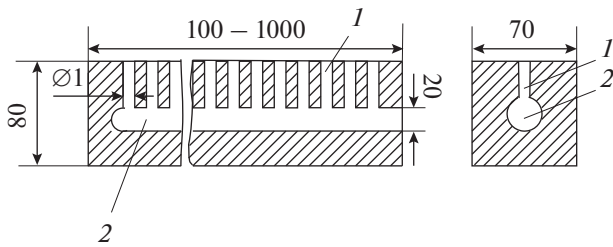


Fig. 3. Extended tuyere design: (1) the shorter gas distribution passage; (2) the main gas distribution passage

As shown by the calculation using equation (10), the refining speed and the NMI content decrease in time. At a residence time of 1/2 seconds, this speed turns constant equal to 0.4% wt./s.

To confirm the theoretical calculations, we conducted industrial tests for defining the optimal gas consumption with the metal blowoff through an extended tuyere (Fig. 3). This allowed selecting the most efficient conditions for refining in the pony ladle of the converter shop on the 60-ton pony ladle of the double-strand CC machine. For the industrial test pattern, see Fig. 4.

In practice, the argon bubble size is dependent from the refractory opening size in which the inert gas is blow in. Thus, a major factor of implementing the inert gas blowoff of metal in the pony ladle is the application of blowoff tuyeres with small gas-release passages. The requirements on the performance properties of these blocks are fairly tough for they are used in extremely severe conditions attended by a long-time contact with liquid metal, heat shifts, contact-induced mechanical influences, etc. A factor no less important for the industrial application of blowoff tuyeres is their stable gas permeability throughout the entire blowoff period in the pony ladle and the possibility of varying the gas consumption level at blowoff.

The blowoff tuyere is designed as a beam with passages that release the gas along the entire length. Thus, it is recommended to use blowoff devices with a small gas discharge opening for the blowoff in bubble mode.

During the metal treatment in the pony ladle outside the kiln, the liquid steel melt is covered with slag, which intensifies the stirring of metal at the liquid steel melt-slag phase boundary. An increased phase stirring intensity and a large contact area favor a more complete reaction behavior and allows using the slag much more efficiently. The contact surface area increases through the formation of a slag-metal emulsion at the contact phase boundary as a result of gas bubbles' penetrating the phase boundary. Thus, the metal carry-over to the slag phase and of slag particles to metal occurs by direct or indirect dispersion. The metal particles with attached NMIs are carried by gas bubbles. Then, a bubble blows in the slag phase and the NMI

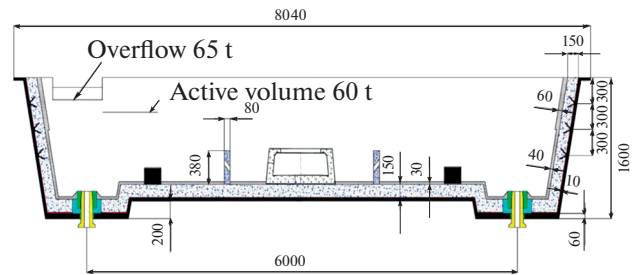


Fig. 4. Layout of the slab CC machine used at the Mariupol Ilyich Iron and Steel Works

particles are adsorbed, which facilitates the NMI elimination from steel.

At large amounts of neutral gas spent on the blowoff through the ladle bottom above the blowoff device, a dynamic gas-liquid region is formed that favors the formation of a so-called open-eye region and creates a circulating stream of metal in the ladle. The open-eye region is a surface on the metal mirror with no slag. A high gas consumption favors the formation of this surface and the neighboring layer that consists of single slag droplets that can be engaged in the liquid metal bath fairly easily with descending and horizontal streams, which thus play the role of an additional NMI source.

The theoretical calculations were checked by comparative tests using extended tuyeres, where test output heats were cast on the 60-ton pony ladle of the double-strand CC machine at the Mariupol Ilyich Iron and Steel Works. The tests were aimed at defining the amount and composition of NMIs in continuously cast slab and ready-made mill products.

The final mounting of the pony ladle was followed by the argon feed upon reaching the level corresponding to about 40 tons of liquid metal. The argon was consumed at 5, 9, 12, and 15 L/min at a pressure of six atmospheres. The industrial tests were conducted on BVA steel slab with a section of 200 × 1245 mm.

The NMI content was estimated according to ASTM EN 45-05 by technique A according in which impurities are divided into four categories by their morphology and into two subcategories by their width and diameter (thin and thick). Impurities are characterized by size, shape, concentration, and distribution but not by chemical composition. Although their composition is not indicated, the standard impurities refer to one of several categories related to their composition (sulfides, oxides, and silicates; the latter are viewed as a type of oxides). The code designations are as follows: type A is for sulfides, type B is for alumina, type C is for silicates, and type D is for globular oxides.

Technique A consists in defining the worst field, that is, the one with the highest score, for each type of impurities of both series, thick and thin; in this case, technique A produces a broader picture of the metal's pollution with large NMIs. For the results of estimat-

Table 1. Results of estimating NMI content by technique A

Argon consumption, l/min	NMI score	Type A		Type B		Type C		Type D		
		thin	thick	thin	thick	thin	thick	thin	thick	impurity diameter, μm
15	Average score	0.58	0.17	0.58	0	0	0	1.0	0	4.42
	Highest score	1.0	1.0	2.5	0	0	0	1.0	0	5.08
13	Average score	1.75	0	1.08	0	0	0	1.0	0	3.06
	Highest score	2.5	0	2.5	0	0	0	1.0	0	5.08
12	Average score	0.5	0	1.0	0	0	0	0.5	0	1.62
	Highest score	0.5	0	1.5	0	0	0	0.5	0	4.08
10	Average score	0.5	0	0.33	0	0	0	0.5	0	1.7
	Highest score	0.5	0	1.0	0	0	0	0.5	0	4.9
9	Average score	1.17	0.58	1.33	0.17	0	0	1.0	0.42	2.87
	Highest score	1.5	2.0	2.0	0.33	0	0	1.0	1.5	4.9
5	Average score	1.83	0.08	0.67	0.19	0	0	1.0	1.17	1.86
	Highest score	3.0	0.5	2.0	0.4	0	0	1.0	2.0	5.08

ing NMIs (for the 10-mm sheet thickness) by technique A along the scales of EN 45-05, see the Table 1.

According to the industrial test data, the best results of eliminating NMIs from the metal are attained at a gas consumption of 10 to 12 L/min. That said, the rolled plates of argon slabs blown off at this rate are purer in terms of sulfide, string alumina, and globular 1D oxide content. The test and the reference metal slab sheets blown off with argon consumed at five to nine l/min show almost no difference in pollution with large globular oxides, which is due to the insufficient stirring of metal and slag at the metal–slag boundary.

The high NMI content in the test metal specimens sharply rises at a gas consumption from 13 to 15 L/min, which is conditioned by the active stirring of metal and slag, which leads to the NMI capture by convective streams of metal

CONCLUSIONS

An extended residence time of a metal droplet in the slag phase is favorable to refining the metal from NMIs. This time ranges from 0.1 to 0.6 seconds, whereas the average refining speed ranges from 0.27 to 0.3% wt. per second. The metallographic tests have confirmed that the best refining results are achieved at a gas consumption from 10 to 12 l/min.

REFERENCES

- Huang, J., Yuan, Z., Shi, S., et al., Flow characteristics for two-strand tundish in continuous slab casting using PIV, *Metals*, 2019, no. 9, pp. 41–52.
- Gushchin, V.N. and Ul'yanov, V.A. Improved tundish 1 refining of steel in continuous-casting machines, *Steel Transl.*, 2017, vol. 47, no. 5, pp. 320–324.
- Dubodelov, V.I., Smirnov, A.N., Efimova, V.G., et al., *Gidrodinamicheskie i fiziko-khimicheskie protsessy v promezhutochnykh kovshakh dlya nepreryvnogo lit'ya stali* (Hydrodynamic and Physicochemical Processes in Tundish for Continuous Steel Casting), Kyiv: Naukova Dumka, 2018.
- Sahai, Y. and Emi, T., *Tundish Technology for Clean Steel Production*, Singapore: World Scientific, 2008.
- Smirnov, A.N., Efimova, V.G., Verzilov, A.P., and Maksaev, E.N., Clogging of submersible nozzles in continuous slab-casting machines, *Steel Transl.*, 2014, vol. 44, no. 11, pp. 833–837.
- Smirnov, A.N., Efimova, V.G., and Kravchenko, A.V., Flotation of nonmetallic inclusions during argon injection into the tundish of a continuous-casting machine. Part 1, *Steel Transl.*, 2013, vol. 43, no. 11, pp. 673–677.
- Smirnov, A.N., Efimova, V.G., and Kravchenko, A.V., Flotation of nonmetallic inclusions during argon injection into the tundish of a continuous-casting machine. Part 2, *Steel Transl.*, 2014, vol. 44, no. 1, pp. 11–16.
- Smirnov, A.N., Kuberskii, S.V., Smirnov, E.N., et al., Influence of meniscus fluctuations in the mold on crust formation in slab casting, *Steel Transl.*, 2017, vol. 47, no. 7, pp. 478–482.

9. Solhed, H., Jonsson, L., and Jönsson, P., A theoretical and experimental study of continuous-casting tundishes focusing on slag-steel interaction, *Metall. Mater. Trans. B*, 2002, vol. 33, no. 2, pp. 173–185.
10. Linzer, B., Rimnac, A., Bragin, S., and Yang, B., AHSS production with Averdi ESP: a new door of opportunity opens, *Proc. METEC Conf. and Trade Fair and 2nd European Steel Technology and Application Days (ESTAD), Düsseldorf, June 15–19, 2015*, Düsseldorf, 2015, p. 290.
11. Brooks, G., Pan, Y., Subagyo, and Coley, K., Modeling of trajectory and residence time of metal droplets in slag-metal-gas emulsions in oxygen steelmaking, *Metall. Mater. Trans. B*, 2005, vol. 36, no. 4, pp. 525–535.
12. Yang, G., Yang, Wang, X., et al., Influence of reoxidation in tundish on inclusion for Ca-treated Al-killed steel, *Steel Res. Int.*, 2013, vol. 85, pp. 784–792.
13. Holappa, L. E., Louhenkilpi, S., and Nurmi, S., Role of slags in steel refining: Is it really understood and fully exploited? *Rev. Métall.*, 2009, vol. 106, no. 1, pp. 9–20.
14. Mabentsela, A., Numerical and physical modeling of tundish slag entrainment in the steelmaking process, *J. Min. Metall., Sect. B*, 2017, vol. 117, no. 5, pp. 469–483.
15. Zhang, L., Thomas, B.G., Wang, X., and Cai, K., Evaluation and control of steel cleanliness—revive, *Proc. 85th Steelmaking Conf.*, Warrendale, PA: Iron Steel Soc., 2002, pp. 431–452.

Translated by S. Kuznetsov

SPELL: 1. ok